Observation of strong direct-like oscillator strength in the photoluminescence of Si nanoparticles

A. Smith, Z. H. Yamani,* N. Roberts, J. Turner, S. R. Habbal,[†] S. Granick, and M. H. Nayfeh[‡] Department of Physics, University of Illinois at Urbana-Champaign, 1110 W. Greeen Street, Urbana, Illinois 61801, USA (Received 18 November 2004; revised manuscript received 20 September 2005; published 7 November 2005)

We have performed time-resolved photoluminescence measurements on suspensions of silicon nanoparticles using near-infrared two-photon femtosecond excitation. Our results for 1 nm particles show wide bandwidth but indicate full conversion to directlike behavior, with a few nanosecond time characteristic, corresponding to oscillator strength comparable to those in direct semiconductors. In addition to fast nanosecond decay, the photoluminescence from 2.85 nm nanoparticle suspension exhibits considerably slower decay, consistent with a transition regime to directlike behavior. The quantum yield is measured to be \sim 0.48, 0.82, and 0.56 for excitation at 254, 310 and 365 nm, respectively, for the blue 1 nm particles, and \sim 0.22, 0.36, and 0.50 for the red 2.85 nm particles. The directlike characteristics are discussed in terms of localization on radiative deep molecularlike Si-Si traps with size-dependent depth.

DOI: 10.1103/PhysRevB.72.205307

I. INTRODUCTION

The prospect of using Si nanocrystals as a gain medium for lasers was conjectured as early as 1990, when visible (red) luminescence in porous silicon was first discovered by Canham.^{1,2} The use of bulk Si and other indirect bandgap semiconductors as a gain medium is problematic. In those, stimulated emission is very weak because the luminescence decay rate is very slow with very weak oscillator strength. Moreover, the loss due to nonradiative Auger processes and free-carrier absorption is very significant, exceeding the gain by stimulated emission. But, the situation is different for ultrasmall particles since they acquire numerous novel characteristics. As the material size is reduced to a few nanometers (~3 nm, for example), quantum confinement, phononexciton coupling, valence band orbital degeneracy, electronhole spin exchange interaction, valley orbit interaction, and optical selection rules experience modifications that strongly impact the electronic and optical activity. A further decrease in the particle size to an ultrasmall regime (1-3 nm, or 20 to 1000 atoms) intensifies the effect of boundaries, resulting in the loss of elasticity and translational symmetry. Under these conditions, both the absorption and gain characteristics of nanocrystallites become heavily dependent on their size.^{3–5}

There have been no measurements of the time dynamics and oscillator strength of the photoluminescence of specific Si cluster configurations in the 1–3 nm size regime. Experimental measurements of the time dynamics in porous silicon have been, however reported² Under some conditions, fast decay channels have been reported. However, the conditions on sample preparation and measurements are not reproducible; and the analysis is not straightforward because porous Si consists of interconnected wirelike structures of random size and shape, with nanostructures being mostly larger than 3 nm. Thus, fabricating size-, shape-, and orientationcontrolled luminescent Si nanoparticles, with reproducibility, would alleviate these problems, and provide an opportunity to elucidate the transition regime under straightforward measurements and interpretation.⁶ In this paper, we present the time dependence of the photoluminescence of suspensions of 1 nm blue luminescent nanoparticles and 2.85 nm red luminescent nanoparticles, 7-9 under two-photon near-infrared PACS number(s): 73.22.-f, 78.67.Bf, 78.47.+p

femtosecond excitation. The particles were prepared using an electrochemical etching method, ¹⁰ which we developed for the dispersion of bulk crystalline Si into identical nanoparticles. ¹¹ Our results for 1 nm particles demonstrate the conversion to directlike behavior with fast decay channels of a few nanosecond time characteristics, corresponding to oscillator strength comparable to those in direct semiconductors. In addition to fast nanosecond decay channels, the photoluminescence from 2.85 nm nanoparticles exhibit considerably slower decay channels, indicating a transition regime from indirect- to directlike behavior. The directlike response is discussed in terms of luminescence from novel size-dependent Si-Si deep traps, with molecularlike localization. ^{5,12–14} The photoluminescence band remains wide, extending over the range 50–70 nm, characteristic of electronic transitions in molecules.

II. EXPERIMENT

We used electrochemical etching in HF and $\rm H_2O_2$ to disperse crystalline Si into ultrasmall nanoparticles. ^{10,11} The wafer is laterally anodized while being advanced slowly into the solution. Because HF is highly reactive with silicon oxide, $\rm H_2O_2$ increases the etching rate, producing smaller particles. Moreover, the oxidative nature of the peroxide produces chemically and electronically high-quality samples. The pulverized wafer is then transferred to an ultrasound bath, under which the film dislodges into a colloidal suspension of nanoparticles. High-resolution TEM shows that, under certain conditions, we produce a family of discrete, nearly spherical nanoparticles, which include 1 and 2.85 nm nanoparticles that can be subsequently separated and purified. ¹⁵

The excitation employs a two-photon process at 760–800 nm, corresponding to an effective single photon process at 380–400 nm. We used a mode-locked femtosecond Tisapphire near-infrared laser system, generating pulses of <150 fs duration at a repetition rate of 80 MHz (12 ns duty cycle). At the target, the average power, 20 mW, is focused to a beam waist of \sim 0.5 μ m, giving an average intensity of 10^7 W/cm² (peak pulse intensity of 10^{12} W/cm²). In the measurement of the time dynamics we did not employ wave-

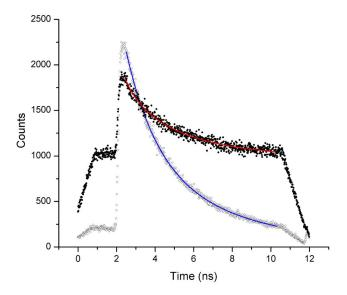


FIG. 1. (Color online) Time-resolved photoluminescence under two-photon process excitation of 2.85 nm (gray) and 1 nm (dark) Si nanoparticles using a femtosecond laser at 780 nm wavelength pulses of <150 fs duration at a repetition rate of 80 MHz (12 ns duty cycle). The solid lines are exponential fits.

length resolution; all of the photoluminescence in the blue band of the 1 nm particles or in the red band of the 2.85 nm particles was collected using a photomultiplier.

III. RESULTS

We prepared a colloid of 1.0 nm nanoparticles. The luminescence band extended from 400-480 nm under excitation in the 760-800 nm range. Measurements of several samples were taken, with good reproducibility, indicating the consistency of the samples of nanoparticles. Moreover, we found no dependence of the decay characteristics on pumping power or particle concentration. The photoluminescence spectra over a wider range of excitation were recently studied using a single photon excitation. The particle exhibits several luminescence bands of emission. The spectra are given in Fig. 2 of both Refs. 6, for example. In these measurements, the excitation wavelength was varied between 250 and 400 nm, while collecting the emission in the range 250-600 nm at each excitation wavelength. Distinct emission bands are observed, centered at 310, 360, and 390 nm. The corresponding excitation bands for these emission wavelengths are centered at 275, 310, and 335 nm (4.6, 4.0, 3.7 eV), respectively. For both the emission and excitation, the bands are \sim 40–70 nm wide.

Figure 1 gives time-resolved photoluminescence in a typical trace. It was taken under 780 nm excitation. The working range of the free decay is \sim 2–11 ns within the 0–12 ns duty cycle. The flat steady-state background the free decay is riding on is due to accumulation resulting from decay rates with a long characteristic time scale. Figure 1 shows that the background is \sim 10% of the maximum yield. This value of background shows that the 1 nm nanoparticle has predominantly short lifetimes <12 ns. We analyze the time dynamics

to a single exponential function and a constant that may account for any decay with a long time characteristic. The procedure yields 2.6±0.3 ns for the lifetime. We next analyzed the decay to multiple decay rates. For two rates, we get lifetimes of 1 and 3 ns with amplitude branching ratios of 1 to 4 and a 5% constant. Measurements using 800 nm excitation gave 1 and 3 ns with 1 to 4 amplitude ratio and 6% constant. Measurements using 760 nm excitation gave 1 and 3 ns with 1 to 4 amplitude ratio and 7% constant. The variation of rates with wavelength is insignificant. Setting the constant to near zero, the fit gives rates of 1.6 and 6 ns with an amplitude ratio of 1.3 to 1. To get an estimate for the oscillator strength of the transition, we use a representative lifetime value of 2.6 ns. The oscillator strength, f, is related to the lifetime τ according to $f=1.5\times 10^{-16}~\lambda^2~(g_b/g_a)/\tau$, where λ is the average luminescence wavelength, in angstroms, and τ is in seconds. g_b/g_a is the ratio of the degeneracy of the ground and excited states.¹⁶ In our experiment, the degeneracy ratio is unknown, since there is no information about the excited state channel(s) responsible for the photoluminescence. If we use a reasonable ratio of one, and use 4000 Å for the wavelength, the expression yields a large oscillator strength of 0.92. Even a degeneracy ratio of 0.33 yields oscillator strengths of 0.3. For comparison, the H_{α} Lyman transition is known to have a large oscillator strength of $\sim 0.4^{17}$ The oscillator strength is a measure of the radiative strength of transitions. In general, in a Z-electron system, the oscillator strength ranges between zero, for no transition, and Z for a fully allowed (strong transition). In a 1 nm nanoparticle there are six dimers that can cause radiative transitions.

We examined a suspension of 2.85 nm nanoparticles. We used chromatography to separate and purify the sample to ensure no contamination from blue luminescent particles or any other species. The purified particles exhibit a red luminescence band, extending from 550–680 nm with a peak near 610 nm with no luminescence in the blue range. The photoluminescence spectrum was recently studied over a wider range of excitation using a single photon excitation. Unlike the 1 nm particle, the 2.85 nm particle does not exhibit multiple luminescence bands; it exhibits only a red band. (See Fig. 7 of Ref. 18 for an example.)

The typical time-resolved photoluminescence of these particles was shown above in Fig. 1. The fluorescence in this case decays to the near 50% level within the detection time window (12 ns). This implies that the nanoparticle has fast decay channels as well as considerably slower decay channels with times >12 ns. Analyzing the time dynamics using two-exponential functions and a constant level gives 1.3 and 5.7 ns with an amplitude ratio of 1 to 1.5 and a constant of 50% of the maximum yield. We are unable to measure the slow decay component with the present system. To get a rough idea of the order of magnitude of the long decay, we set the constant to near zero. In this case the fit gives rates of 1.6 and 38 ns with amplitudes of 1 to 2.

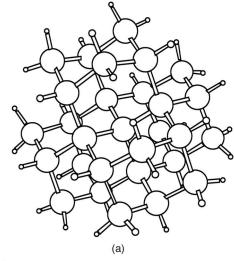
We made quantum yield measurements using a research grade commercial polysilicon solar sheet. The response of the sheet is known as a function of the wavelength of the incident radiation. We spread the nanoparticles into a thin film on the active surface, and measured the efficiency of the cell as a function of the thickness of the nanoparticle film.

By comparing the response at zero thickness with that for nearly full absorption of the UV in the nanofilm, we derived the conversion efficiency of the UV into visible radiation. For the 1 nm particles we arrive at a quantum yield of \sim 0.48, 0.82, and 0.56 for excitation at 254, 310, and 365 nm, respectively. The 2.85 nm red particles exhibit for the same excitations a yield of \sim 0.22, 0.36, and 0.5, respectively. These large quantum yields are also consistent with emission intensity yields. In a previous work, we were able to measure the emission intensity from single 1 nm particles excited by the two-photon process at 780 nm. This is consistent with a large quantum yield, and sizable absorption. (See Ref. 11.)

IV. DISCUSSION

The recombination of spatially confined excitons in the bulk of nanocrystals, analyzed by Hybertsen using an effective mass procedure,³ shows that for sizes smaller than 1.5-2.0 nm, the oscillator strength of zero-phonon transition dominates that of phonon-assisted transitions. In this size regime, losses due to nonradiative processes drop. However, the luminescent excitons are found to have an oscillator strength of 0.002 in nanocrystallites of 1.5 nm diameter corresponding to the luminescence lifetime of a few microseconds. Sundholm obtained an oscillator strength of 0.0017 for luminescence from a fully nonreconstructed bulk Si₂₉ (1 nm) cluster configuration [see Fig. 2(a)].^{4,9} In those calculations, the molecular structures of the ground and the lowest excited state, hence the electronic absorption and emission energy were optimized at the density-functional-theory (DFT) level using the time-dependent perturbation theory (TDDFT) approach. Other calculations of spherical clusters⁵ used linear combination of atomic orbital framework. The calculations showed that the nature of the transition, i.e., Al-T₂, T₂-T₂, or $E-T_2$ in the representation of the T_d point group, can change quickly with respect to a small change in the crystallite size. In the range of 1.3–1.5 nm diameter, for instance, the calculation gives oscillating rates of recombination that span over two decades (10^6-10^8 Hz) , which correspond to a 0.001-0.1 range of oscillator strength, with the upper limit approaching our experimental result.

A viable explanation of the fast decay rates observed involves molecularlike traps. If the trap states are shallow states, the picture will not essentially change.³ This is due to the fact that shallow trapping changes the zero-phonon and phonon-assisted oscillator strengths in roughly the same way. If only deep traps are really involved in the photoluminescence process and act as a decisive factor, fast decay is expected and little change in oscillator strength with cluster size could be observed. A recent model presented by Allan *et al.* involves intrinsic radiative Si self-traps,¹² which were discovered in density functional theory simulations, and is based on Si-Si surface reconstruction. The wave functions of these states are not extended throughout the bulk of the nanoparticles, but rather concentrated on local sites of atomic dimensions.^{5,12,13} Those reconstructions can take place more



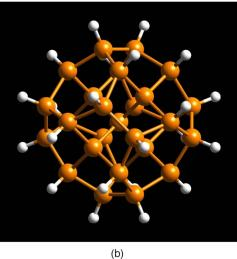


FIG. 2. (Color online) Configurations of 1 nm Si_{29} nanoparticle (a) nonreconstructed $\mathrm{Si}_{29}\mathrm{H}_{36}$. Large silicon atoms. Small hydrogen atoms. (b) Computer prototype of constructed Si_{29} (1 nm) $\mathrm{Si}_{29}\mathrm{H}_{24}$ nanoparticle. "Orange (large) Si atoms; white (small) H atoms."

readily in ultrasmall particles for which the elasticity drops. This makes the atoms amenable to large movement. For instance, in the model, some surface Si atoms in 1 nm particles move by more than 0.65 Å from their bulk positions to reconstruct into novel radiative Si-Si dimers, with a binding energy of 0.75 eV, much larger than the thermal agitation energy of 0.025 eV. But, the binding energy (depth of trap) depends sensitively on the size of the particle, dropping from 0.75 eV for 1 nm to a shallow condition for nanoparticles of a few nanometers diameter. For instance, it is 0.25 eV in 1.7 nm particles, and is expected to be ~ 0.03 eV for 3 nm particles, comparable to the thermal agitation energy. The formation of these reconstructions is favorable under our dispersion conditions. H₂O₂ in our etchant is critical for controlling the amount and configuration of hydrogen on the surface, hence the reconstruction. The reaction Si_nH_m \rightarrow Si_nH_{m-2}+H₂ has a barrier of 0.6 eV. However, the reaction

 $Si_nH_m+H_2O_2 \rightarrow Si_nH_{m-2}+2H_2O$ proceeds followed by reconstruction to form novel radiative Si-Si dimer bonds while gaining an energy of 0.25 eV. The fully reconstructed bulklike Si₂₉ (1 nm) cluster configuration with a total of six dimers is shown in Fig. 2(b). The large binding of the trap may explain the domination of the fast fluorescence decay time in 1 nm particles. But the shallow binding of the trap in a 2.85 nm particle may explain the presence of a fast as well as a slow decay channel. The slow components may be associated with radiative recombination of electron hole pairs in the bulk of the particle, i.e., under spatial bulklike localization in the particle. Allan et al. presented an example of a recombination on traps. Detailed calculations of the oscillator strength or lifetime for transitions in the HOMO-LUMO gap in a 1.67 nm cluster gave lifetimes as short as 100 ns. 12 There is no corresponding calculation for the 1 nm particle, or for the 2.85 nm particle. Such calculations should be most helpful for a detailed comparison with the experimentally observed lifetimes.

The measured fast time dynamics or the derived large oscillator strengths are supported by the sizable quantum yield of nearly 50% reported above for 1 nm particle. The quantum yield of nearly 25% is consistent with the presence of a fast as well as a slow luminescence channel for the red 2.85 nm particles.

It is worth mentioning that Si-Si bonds have been a factor in other systems that exhibited fast nanosecond fluorescence. Pecause of its Si-Si σ conjugation, short silane chains or polysilane have many unique electrical and optical properties. For instance, the measured fluorescence lifetime in polysilane is in the subnanosecond regime, namely 0.4 ns. Moreover, in a wide wavelength range (about 280–350 nm), polysilane displays strong absorption. Upon ultraviolet absorption, it emits strong fluorescence with a quantum efficiency of 0.1–0.8.

Local density theory calculations in the ultrasmall size regime showed that the rate of nonradiative Auger recombination processes in Si clusters drops appreciably such that it becomes dominated by the simultaneously rising rate of radiative recombination.⁵ For instance, for sizes with a band gap larger than 2.2 eV, namely of diameters smaller than 2.85 nm, the nonradiative rate begins to drop rapidly. For 1 nm particles used in this study (a gap of 3.5 eV), the nonradiative rate is vanishing small, while the radiative channel is fast. Thus the ratio of the radiative rate to the sum of the radiative and the nonradiative rates (fluorescence quantum yield) is expected to be large. Our measurement of large oscillator strength implies that channels other than radiative, which may channel the excitation out of the radiative state and decrease the fluorescence intensity, are indeed of little consequence. In this limit, the inverse of the radiative lifetime, hence the oscillator strength is proportional to the integral of its absorption coefficient over the spectrum (Strickler-Berg relation).²¹ In fact in our measurement, the detector integrates all of the photoluminescence in the band. It is to be noted that, despite the directlike time characteristics, the photoluminescence band is wide, characteristic of electronic transitions in molecules, and extending over the range 400-480 nm for 1 nm particles and over 550-680 nm for the 2.85 nm particles.

Optical measurements taken by several groups using Si clusters in various formations showed signatures of optical gain, which point to a fast photoluminescence time characteristic. For instance, the excitation of porous silicon with near-infrared two-photon femtosecond processes resulted in blue luminescence with highly nonlinear characteristics of stimulated emission.²² The excitation of clusters or films of 1 nm silicon nanoparticles with near-infrared two-photon femtosecond processes resulted under certain conditions in directed blue beams.²³ The excitation of clusters of red luminescent 2.85 nm diameter Si nanoparticles with green radiation from a mercury lamp produced directed red beams.²⁴ Optical amplification at the emission wavelength was reported in some measurements in 3 nm luminescent nanocrystals prepared by ion implantation, or by plasmaenhanced chemical vapor deposition.²⁵⁻²⁹

Upon heavy oxidization using a variety of oxidation protocols, the red microsecond luminescence in porous silicon transforms into fast nanosecond (1-10 ns)30,31 blue luminescence. 30-41 The protocols include rapid thermal oxidation (RTO), chemical oxidation, mild oxidation by boiling water, 32,33 amine treatment in combination with RTO, 39 and long-term aging. The red band does not evolve smoothly into the blue band but tends to vanish after heavy oxidation.³⁴ Thus, some researchers believe that this green/blue band is not due to quantum confinement but rather related to the Si-O species,³¹ or due to defects and the silica networks on which OH groups are absorbed. 40 However, an interpretation in terms of quantum confinement in Si clusters that decrease in size upon oxidation has been controversial, especially since the emergence of blue is not a smooth function of the oxidation period. 40,41,34 It is to be emphasized, however, that, after etching, our samples have not been thermally or chemically treated nor oxidized.

V. CONCLUSION

In conclusion, we recorded the time dependence of the photoluminescence of suspension of fluorescent silicon nanoparticles, under two-photon femtosecond excitation. Under a single photon excitation, we measure a quantum yield of nearly 50% for the blue 1 nm particles, and nearly 25% for the red 2.85 nm particles. We find predominantly fast luminescence decay in 1 nm particles, corresponding to large oscillator strength. For larger particles of 2.85 nm diameter, we find both fast nanosecond decay as well as slow decay. The measurements are discussed in terms of a luminescence mechanism that is based on size-dependent intrinsic molecularlike localization on radiative Si-Si traps. The measured time dynamics of photoluminescence for 1 nm particles indicates full conversion to directlike behavior, with few nanosecond time characteristics, corresponding to oscillator strength comparable to those in direct semiconductors. On the other hand, a 2.85 nm nanoparticle suspension exhibits luminescence characteristic consistent with a transition regime to directlike behavior. The luminescence bandwidth remains wide.

The directlike characteristics are discussed in terms of localization on radiative deep molecularlike Si-Si traps with size-dependent depth.

ACKNOWLEDGMENTS

The authors acknowledge U.S. NSF Grants No. ATM 04–50149, and BES-0118053, the State of Illinois Grant IDCCA No. 00-49106, and KFUPM. J.T. and S.G. acknowledge sup-

port by the U.S. Department of Energy, Division of Materials Science and the Frederick Seitz Materials Research Laboratory at the University of Illinois at Urbana-Champaign. J.T. acknowledges support from Colgate-Palmolive.

- *Also at KFUPM, Dhahran, Saudi Arabia.
- [†]Also at IFA, University of Hawaii, Honolulu, HI 96822, USA.
- ‡Electronic address: m-nayfeh@uiuc.edu
- ¹L. T. Canham, Appl. Phys. Lett. **57**, 1046 (1990).
- ² See, for example, the review article: A. G. Cullis, L. T. Canham, and P. Calcott, J. Appl. Phys. **82**, 909 (1997).
- ³M. S. Hybertsen, Phys. Rev. Lett. **72**, 1514 (1994).
- ⁴D. Sundholm, Phys. Chem. Chem. Phys. **6**, 2044 (2004).
- ⁵J. P. Proot, C. Delerue, and G. Allan, Appl. Phys. Lett. **61**, 1948 (1992).
- ⁶S. Rao, J. Sutin, R. Clegg, E. Gratton, M. H. Nayfeh, S. Habbal, A. Tsolakidis, and R. M. Martin, Phys. Rev. B **69**, 205319 (2004); M. Nayfeh, S. Habbal, and S. Rao, Astrophys. J. **621**, L121 (2005).
- ⁷L. Mitas, J. Therrien, G. Belomoin, and M. H. Nayfeh, Appl. Phys. Lett. **78**, 1918 (2001).
- ⁸E. W. Draeger, J. C. Grossman, A. J. Williamson, and G. Galli, Phys. Rev. Lett. **90**, 167402 (2003).
- ⁹D. Sundholm, Nano Lett. **3**, 847 (2003).
- ¹⁰G. Belomoin, J. Therrien, and M. Nayfeh, Appl. Phys. Lett. **77**, 779, (2000); Z. Yamani, H. Thompson, L. Abuhassan, and M. H. Nayfeh, *ibid.* **70**, 3404 (1997); D. Andsager, J. Hilliard, J. M. Hetrick, L. H. Abuhassan, M. Plisch, and M. H. Nayfeh, J. Appl. Phys. **74**, 4783 (1993); Z. Yamani, S. Ashhab, A. Nayfeh and M. H. Nayfeh, *ibid.* **83**, 3929 (1998).
- ¹¹O. Akcakir, J. Therrien, G. Belomoin, N. Barry, E. Gratton, and M. Nayfeh Appl. Phys. Lett. **76**, 1857 (2000).
- ¹²G. Allan, C. Delerue, and M. Lannoo, Phys. Rev. Lett. **76**, 2961 (1996).
- ¹³ M. H. Nayfeh, N. Rigakis, and Z. Yamani, Phys. Rev. B **56**, 2079 (1997); Mater. Res. Soc. Symp. Proc. **486**, 243 (1998).
- ¹⁴G. Belomoin, M. Alsalhi, A. Alaql, and M. H. Nayfeh, J. Appl. Phys. **95**, 5019 (2004).
- ¹⁵G. Belomoin, J. Therrien, A. Smith, S. Rao, R. Twesten, S. Chaieb, L. Wagner, L. Mitas, and M. Nayfeh, Appl. Phys. Lett. 80, 841 (2002).
- ¹⁶M. Weissbluth, in *Atoms and Molecules* (Academic, San Diego, 1978), p. 515.
- ¹⁷H. Bethe and E. Salpeter, *Quantum Mechanics of One and Two Electron Atoms* (Plenum, New York, 1957).
- ¹⁸L. Abuhassan, M. Khanlary, P. Townsend, and M. H. Nayfeh, J. Appl. Phys. **97**, 104314–1 (2005).
- ¹⁹ M. Stupka, M. Nayfeh, and M. Alsalhi, Mater. Res. Soc. Symp. Proc., December 2005.
- ²⁰G. Li, J. Tan, H. Fu, H. Ma, D. Chen, and Z. Zhou, J. Polym. Sci., Part B: Polym. Phys. **78**, 133 (2000); G. Li., D. Chen, F. Bai, and Y. Mo, *ibid.* **34**, 1583 (1996).
- ²¹S. R. Strickler and R. A. Berg, J. Chem. Phys. **37**, 814 (1962).

- ²²M. Nayfeh, O. Akcakir, J. Therrien, Z. Yamani, N. Barry, W. Yu, and E. Gratton, Appl. Phys. Lett. 75, 4112 (1999).
- ²³M. H. Nayfeh, O. Akcakir, G. Belomoin, N. Barry, J. Therrien, and E. Gratton, Appl. Phys. Lett. 77, 4086 (2000).
- ²⁴M. H. Nayfeh, S. Rao, N. Barry, J. Therrien, G. Belomoin, A. Smith, and S. Chaieb, Appl. Phys. Lett. 80, 121 (2002).
- ²⁵L. Pavesi, L. Dal Negro, C. Mazzoleni, G. Franzo, and F. Priolo, Nature 408, 440 (2000); L. Dal Negro, M. Cazzanelli, N. Daldosso, Z. Gaburro, L. Pavesi, F. Priolo, D. Pacifici, G. Franzo, and F. Iacona, Physica E (Amsterdam) 16, 297 (2003); L. Dal Negro, M. Cazzanelli, L. Pavesi, S. Ossicini, D. Pacifici, G. Franzo, F. Priolo, and F. Iacona, Appl. Phys. Lett. 82, 4636 (2003).
- ²⁶L. Khriachtchev, M. Rasanen, S. Novikov, and J. Sinkknen, Appl. Phys. Lett. **79**, 1249 (2001).
- ²⁷ K. Luterova, I. Pelant, I. Mikulskas, R. Tomasiunas, D. Muller, J. J. Grob, J. L. Rehspringer, and B. Honerlage, J. Appl. Phys. **91**, 2896 (2002).
- ²⁸ J. Valenta, I. Pelant, and J. Linnros, Appl. Phys. Lett. **81**, 1396 (2002).
- ²⁹R. G. Elliman, M. J. Lederer, N. Smith, and B. Luther-Davies, Nucl. Instrum. Methods Phys. Res. B **206**, 427 (2003).
- ³⁰ V. Petrova-Koch, T. Muschik, D. I. Kovalev, F. Koch, and V. Lehmann, in *Microcrystalline Semiconductors: Material Science and Devices*, edited by P. M. Fauchet, C. C. Tsai, L. T. Canham, I. Shimizu, and Y. Aoyagi (Material Research Society, Pittsburgh, PA, 1993), Vol. 283, p. 178.
- ³¹L. Tsybeskov, J. V. Vandeshev, and P. M. Fauchet, Phys. Rev. B 49, R7821 (1994).
- ³²X. Y. Hou, G. Shi, W. Wang, F. L. Zhang, P. H. Hao, D. M. Huang, and X. Wang, Appl. Phys. Lett. **62**, 1097 (1993).
- ³³ X. Wang, G. Shi, F. Zhang, W. Wang, P. Hao, and X. Hou, Appl. Phys. Lett. **62**, 2363 (1993).
- ³⁴D. I. Kovalev, I. D. Yaroshetzkii, T. Muschik, V. Petrova-Koch, and F. Koch, Appl. Phys. Lett. 63, 214 (1994).
- ³⁵H. Mimura, T. Futagi, T. Matsumoto, T. Nakamura, and Y. Kanemitsu, Jpn. J. Appl. Phys., Part 1 133, 586 (1994).
- ³⁶P. M. Calcott, K. J. Nash, L. T. Canham, M. J. Kane, and K. Brumhead, J. Phys.: Condens. Matter 5, L91 (1993).
- ³⁷ A. Loni, A. J. Simons, P. D. J. Calcott, and L. T. Canham, J. Appl. Phys. **77**, 3557 (1995).
- ³⁸C. I. Harris, M. Syvajarvi, J. F. Bergman, C. Kordina, A. Henry, B. Monemar, and E. Janzen, Appl. Phys. Lett. 65, 2451 (1994).
- ³⁹G-B. Li, L-S. Liao, X-B. Liu, X-Y. Hou, and X. Wang, Appl. Phys. Lett. **70**, 1285 (1997).
- ⁴⁰H. Tamura, M. Ruckschloss, T. Wirschem, and S. Veprek, Appl. Phys. Lett. **65**, 1537 (1994).
- ⁴¹ M. K. Lee and K. R. Peng, Appl. Phys. Lett. **62**, 3159 (1993).